The crystal structure of gillulyite, Tl₂(As,Sb)₈S₁₃, from the Mercur gold deposit, Tooele County, Utah, U.S.A.

FRANKLIN F. FOIT, JR.

Department of Geology, Washington State University, Pullman, Washington 99164, U.S.A.

PAUL D. ROBINSON

Department of Geology, Southern Illinois University, Carbondale, Illinois 62901, U.S.A.

JAMES R. WILSON

Department of Geology, Weber State University, Ogden, Utah 84408-2507, U.S.A.

ABSTRACT

Gillulyite, $Tl_2(As^{3+},Sb^{3+})_8S_{13}$, is monoclinic with space group $P2/n$ and $a = 9.584(3)$, $b = 5.679(2)$, $c = 21.501(6)$ Å, $\beta = 100.07(2)°$, $V = 1152.2(7)$ Å³, and $Z = 2$. The average structure was determined using direct methods and refined to a final residual of 0.046 using 930 reflections. The structure consists of Tl-As-S- and As-S-bearing sheets, each present statistically 50% of the time. Four sheets, linked together by Tl-S, As-S, and S-S bonds, are stacked parallel to (001), yielding the 21-Å c-axis repeat of the average unit cell. The Tl1 atom within the Tl-As-S sheet is coordinated by six S nearest neighbors, which form a distorted trigonal prism. The partially occupied Tl2 position between the sheets is split symmetrically about the twofold axis with a separation of 1.28 Å and equal but partial occupancies of 25%. The disordering of the Tl2 position and extreme distortion of its coordination polyhedron is probably the result of the Tl^+ $6s^2$ lone pair effect.

The mean bond distances for the AsS_3 pyramids range from 2.263 to 2.319 Å. However, four of five pyramids have a fourth S neighbor at distances ranging from 2.943 to 3.001 Å, which may be rationalized in terms of the As^{3+} $4s^2$ lone pair effect. Edge sharing among the AsS_3 pyramids results in an As-As distance of 2.562 Å, comparable with that observed in elemental As. The presence of S-S and As-As bonding suggests that gillulyite might more appropriately be classified as a sulfide rather than a sulfosalt.

INTRODUCTION

The new mineral gillulyite, $Tl_2(As,Sb)_8S_{13}$, one of several unusual Tl minerals found in the Mercur gold deposit, Utah, was reported by Wilson et al. (1991) to be a new thallium arsenic sulfosalt. The details of the occurrence, composition, optical and physical properties, and powder diffraction and unit-cell data are presented in this earlier work. This paper presents the results of a structural investigation of this unusual mineral.

STRUCTURE DETERMINATION AND REFINEMENT

After considerable searching, an irregular fragment of gillulyite was found that produced relatively narrow and symmetrical diffraction maxima. A hemisphere of data was collected and averaged to yield a more accurate data set. A scan speed of 6°/min (in ω) was used. Weak reflections [$I < 10.0\sigma_I$] were rescanned (maximum of two rescans) and the counts accumulated to improve accuracy. Experimental details are given in Table 1.

Examination of a series of precession photographs confirmed the cell parameters and revealed a weak zone of diffuse and split reflections in the b* direction, which effectively doubles the length of the b axis. These reflec-

tions were too weak to be measured and suggest minor ordering in the b direction that was not investigated.

Systematic absences indicate the space group to be Pn or $P2/n$. Intensity statistics support the latter choice, which was confirmed by the successful solution and refinement of the structure. The severe effects of absorption were corrected by the empirical Ψ-scan method. Direct methods produced solutions that showed what appeared to be AsS_3 groups in a linked pattern, but the expected large peaks representing the Tl atoms were absent; thus, these solutions were considered to be false. Only after many attempts with various direct and heavy atom methods were we able to decipher the highly disordered average structure described below, with its partially occupied As, S, and Tl positions. In hindsight, we realize that the direct methods program Mithril (Gilmore, 1984) had produced correct locations for most of the atoms early in the structure determination process, but we were initially unwilling to accept them. The remaining atomic sites were found by difference-Fourier syntheses.

Full-matrix, least-squares refinement was performed to minimize $\Sigma w(|F_o| - |F_c|)^2$. All computer programs used were from Texsan (Molecular Structure Corporation, 1985). Atomic scattering factors and anomalous disper-

sion corrections were taken from the *International Tables for X-ray Crystallography* (Ibers and Hamilton, 1974). A site occupancy refinement of the As positions indicated that virtually all the Sb found in the microprobe analyses of gillulyite (Wilson et al., 1991) resides at the As4 and As5 sites; the refined occupancy values are in good agreement with the electron microprobe analytical values. Table 2 lists the final refined positional, occupancy, and displacement parameters; bond distances and angles are presented in Table 3. The observed and calculated structure factors are given in Table 4.[1]

The presence of the weak and diffuse superstructure reflections, which double the length of b, abnormally large Tl and S thermal parameters, a split Tl2 position, and partial site occupancies reveal the existence of domains and partial atom ordering in gillulyite. Thus, what was determined and is described below is the average structure.

DISCUSSION

General structural details

The structure of gillulyite is a composite of two types of structurally similar sheets, Tl1-As-S-bearing and As-S-bearing sheets situated parallel to (001). Each of the two sheet types is present statistically 50% of the time. The first type (Fig. 1) consists of single chains of edge-sharing Tl1-S_6 polyhedra extending parallel to [010] and isolated three-membered rings, As1, As2, and As3, of corner-sharing AsS$_3$ pyramids. The isolated As$_3$S$_4$ rings are sutured together by edge sharing with Tl1 polyhedra in adjacent chains. Tl1 is coordinated by six S atoms forming a distorted trigonal prism, with one side parallel to (001) and the prism axis parallel to [100]. The Tl1-S distances range from 3.300 to 3.438 Å, with a mean of 3.356 Å (Table 3). The next nearest S neightbors are S4 at distances of 3.915 and 3.983 Å. Tl polyhedral edges shared with adjacent As and Tl polyhedra are the short-

[1] To obtain a copy of Table 4, order Document AM-95-582 from the Business Office, Mineralogical Society of America, 1130 Seventeenth Street NW, Suite 330, Washington, DC 20036, U.S.A. Please remit $5.00 in advance for the microfiche.

TABLE 1. Experimental details for gillulyite

Crystal data	
Tl$_2$(As$_{7.78}$,Sb$_{0.22}$)S$_{13}$	$V = 1152.2(7)$ Å^3
$M_r = 1435.20$	$Z = 2$
Monoclinic	$D_x = 4.14$ g/cm
$P2/n$	$D_o = 4.02$ g/cm
$a = 9.584(3)$ Å	MoKα
$b = 5.679(2)$ Å	$\lambda = 0.71069$ Å
$c = 21.501(6)$ Å	$\mu = 265.59$ cm^{-1}
$\beta = 100.07(2)°$	$T = 296$ K
Cell parameters from	irregular fragment
20 refl.	$0.22 \times 0.14 \times 0.10$ mm
$2\theta = 43.5$–$49.1°$	red
Data collection	
Rigaku AFC5S diffractometer	930 observed refl. [$I > 4\sigma_I$]
Absoprtion correction	$2\theta_{max} = 50°$
Ψ scan empirical	$h = -11$–11
4 refl.	$k = 0$–6
$T_{min} = 0.48$, $T_{max} = 1.0$	$l = -25$–25
4504 measured refl.	3 standard refl.
2031 independent refl.	frequency: 150 refl.
	intensity variation: 1.4%
Refinement	
Refinement on F	$w = 4F_o^2/\sigma_{F_o^2}^2$
Final $R = 0.046$	127 parameters
$R_w = 0.061$	$(\Delta/\sigma)_{max} = 0.001$
$S = 1.57$	$(\Delta\rho)_{max} = 3.83$ e/Å^3
930 refl.	$(\Delta\rho)_{min} = -2.05$ e/Å^3

est, and the Tl-S bonds to the bridging S are alternately long and short parallel to the chain length (Table 3, Fig. 2). Despite having a lower coordination number (6), the mean Tl1-S distance is larger than that observed for [8]Tl (3.339 Å) in bernardite, TlAs$_5$S$_8$ (Pašava et al., 1989), [7]Tl (3.294 Å) in lorandite, Tl$_2$As$_2$S$_4$ (Fleet, 1973), and [7]Tl (3.288 Å) in fangite (Wilson et al., 1993). Abnormally long mean bond distances (e.g., [6]Tl2-S = 3.445 Å) and anomalously high isotropic displacement parameters (B_{iso} ~ 5) were also observed for the partially occupied Tl positions in the averaged structure of imhofite (Divjaković and Nowacki, 1976).

Two of the three pyramidal AsS$_3$ groups (As1 and As3) that comprise the three-membered rings have only As-S bridge bonds, and these range from 2.289 to 2.359 Å (mean = 2.319 Å) and 2.294 to 2.352 Å (mean = 2.318 Å), respectively. These means are almost identical to the average bridge bond (2.31 Å) observed in well-refined sulfosalt structures (Takéuchi and Sadanaga, 1969). The

TABLE 2. Atomic coordinates, anisotropic displacement parameters, and B equivalents for gillulyite

	x	y	z	Occup.	U_{11}	U_{22}	U_{33}	U_{12}	U_{13}	U_{23}	U_{eq}
Tl1	0.8102(3)	0.9483(5)	0.1488(1)	0.5	0.035(1)	0.035(1)	0.066(2)	-0.004(1)	0.024(1)	-0.008(1)	0.044(1)
Tl2	0.1895(4)	0.8829(6)	0.2589(2)	0.5	0.130(4)	0.052(2)	0.125(3)	-0.009(2)	-0.077(4)	-0.004(2)	0.114(2)
As1	0.4732(2)	0.4472(4)	0.0883(1)	1.0	0.010(1)	0.013(1)	0.021(1)	0.001(1)	0.0023(8)	0.002(1)	0.015(1)
As2	0.2587(2)	0.9009(5)	0.0205(1)	1.0	0.019(1)	0.025(2)	0.029(1)	0.003(1)	0.008(1)	0.014(1)	0.024(1)
As3	0.0965(2)	0.4476(5)	0.0883(1)	1.0	0.011(1)	0.014(1)	0.023(1)	-0.000(1)	0.0069(9)	0.001(1)	0.016(1)
As4, Sb1	0.8077(5)	0.2107(8)	0.1446(2)	0.43, 0.07	0.015(3)	0.016(3)	0.016(2)	0.001(2)	0.008(2)	0.002(2)	0.015(1)
As5, Sb2	0.8087(5)	0.6617(8)	0.1468(2)	0.46, 0.04	0.017(3)	0.014(2)	0.015(2)	-0.002(2)	0.006(2)	0.002(2)	0.015(1)
S1	0.3105(6)	0.388(1)	0.1543(3)	1.0	0.009(3)	0.025(4)	0.030(3)	0.002(3)	0.007(2)	0.009(3)	0.021(2)
S2	0.6452(5)	0.437(1)	0.1813(2)	1.0	0.015(3)	0.024(3)	0.018(3)	0.001(3)	0.009(2)	-0.002(3)	0.018(2)
S3	0.4708(7)	0.850(1)	0.0876(3)	1.0	0.019(3)	0.014(4)	0.051(4)	-0.004(3)	0.001(3)	0.000(3)	0.029(2)
S4	0.2435(6)	0.543(1)	-0.0191(3)	1.0	0.023(3)	0.052(4)	0.018(3)	0.005(4)	0.010(2)	-0.004(3)	0.030(2)
S5	0.0980(7)	0.852(1)	0.0879(3)	1.0	0.028(3)	0.023(3)	0.031(3)	0.001(3)	0.013(3)	-0.002(3)	0.026(2)
S6	0.9980(5)	0.434(1)	0.1811(2)	1.0	0.012(3)	0.027(3)	0.018(3)	-0.004(3)	0.009(2)	0.000(3)	0.018(2)
S7	0.844(1)	0.941(2)	0.2254(5)	0.5	0.028(6)	0.019(6)	0.013(5)	0.007(6)	0.005(4)	0.001(5)	0.020(3)

TABLE 3. Bond distances (Å) and angles (°) for gillulyite

Atoms	Distance	Atoms	Distance	Angles
Tl1-S5^A*	3.300(7)	S2-S3	3.344(9)	59.2(2)
Tl1-S6^B	3.302(7)	S2^B-S3	4.095(9)	75.9(2)
Tl1-S2^B	3.327(7)	S2-S6	3.383(8)	58.9(1)
Tl1-S3	3.335(7)	S2^B-S6^B	3.383(8)	61.4(2)
Tl1-S6	3.437(7)	S5^A-S6^B	4.068(9)	76.1(2)
Tl1-S2	3.438(7)	S5^A-S6	3.349(9)	59.6(2)
Tl1-S4^C	3.915(8)	S6-S6^B	5.679(2)	114.8(2)
Tl1-S4^D	3.983(8)	S2-S2^B	5.679(2)	114.2(2)
Mean**	3.356	S3-S5^A	6.01(1)	129.9(2)
Tl2-S7^E	3.280(10)			
Tl2-S1^F	3.374(8)			
Tl2-S6^E	3.404(7)			
Tl2-S1^G	3.421(7)			
Tl2-S5^F	3.560(8)			
Tl2-S5	3.633(8)			
Tl2-S6^H	3.860(7)			
Tl2-S3^F	3.879(10)			
Tl2-S1	3.902(8)			
Tl2-S1^B	3.942(7)			
Tl2-S6^I	3.971(7)			
Mean**	3.445			
As1-S3	2.289(7)	S1-S2	3.170(8)	85.5(2)
As1-S1	2.309(6)	S1-S3	3.475(9)	98.2(3)
As1-S2	2.359(5)	S1-S4	3.777(8)	91.0(2)
As1-S4	2.950(8)	S2-S3	3.344(9)	92.0(2)
Mean†	2.319	S2-S4	5.287(8)	169.6(2)
Grand mean	2.477	S3-S4	3.362(9)	78.7(2)
As2-S4	2.197(8)	S3-S5	3.57(1)	101.8(3)
As2-S3	2.296(7)	S4-S3	3.362(9)	96.8(3)
As2-S5	2.309(7)	S4-S5	3.381(9)	97.2(3)
Mean	2.267			
As3-S5	2.294(7)	S1-S4	3.777(8)	90.8(2)
As3-S1	2.307(6)	S1-S6^E	3.158(8)	85.3(2)
As3-S6^E	2.352(5)	S5-S1	3.480(9)	98.3(2)
As3-S4	2.959(8)	S5-S4	3.381(9)	79.0(2)
Mean†	2.318	S5-S6^E	3.349(9)	92.2(2)
Grand mean	2.478	S6^E-S4	5.291(8)	169.8(2)
As4-S6	2.248(7)	S6-S2	3.383(8)	97.1(3)
As4-S2	2.264(8)	S6-S7^J	3.38(1)	96.1(4)
As4-S7^J	2.296(10)	S6-S4^C	3.83(1)	92.6(2)
As4-S4^C	3.001(8)	S2-S7^J	3.44(1)	97.9(4)
Mean†	2.269	S2-S4^C	3.82(1)	92.0(2)
Grand mean	2.452	S7-S4^C	5.26(1)	165.9(4)
As5-S6	2.244(8)	S2-S4^C	3.822(8)	93.9(2)
As5-S2	2.246(7)	S2-S7	3.48(1)	99.9(4)
As5-S7	2.299(10)	S6-S2	3.383(8)	97.8(3)
As5-S4^C	2.943(7)	S6-S4^C	3.831(8)	94.2(2)
Mean†	2.263	S6-S7	3.45(1)	98.4(4)
Grand mean	2.433	S7-S4^C	5.16(1)	159.7(4)
As4-As5	2.562(6)			
S7-S7^I	2.24(2)			
T12a-T12b^F	1.28(1)			

Note: symmetry operators are as follows: A = x + 1, y, z; B = x, y + 1, z; C = $-x$ + 1, $-y$ + 1, $-z$; D = $-x$ + 1, $-y$ + 2, $-z$; E = x − 1, y, z; F = ½ − x, y, ½ − z; G = ½ − x, y + 1, ½ − z; H = x − 1, y + 1, z; I = ¾ − x, y, ½ − z; J = x, y − 1, z.

* S7 is not included as part of Tl1 coordination polyhedron because S7, like As4 and As5, is statistically present only 50% of the time and is assumed to be present only in the As-S sheets. The validity of this assignment is confirmed by the fact that one of the Tl1-S7 distances (3.302 and 1.623 Å) is unreasonably short.
** Average of six shortest bonds.
† Average of three shortest bonds.

Fig. 1. The Tl1-As-S sheet projected down [001] showing the chain of edge-sharing TlS₆ polyhedra extending parallel to [010] and the isolated three-member rings of corner-sharing AsS₃ pyramids. The large black circles are Tl, the small gray spheres are As, and the large lightly shaded spheres are S. The unit cell is outlined.

As2S₃ pyramid has two bridge bonds comparable in length with those observed in the other AsS₃ pyramids and one short nonbridge bond, As2-S4, of a length (2.197 Å) comparable with the nonbridge bonds observed in sulfosalt structures. S4 is only 2.950 Å from As1 and 2.959 Å from As3, and thus it might be argued that they are fourfold
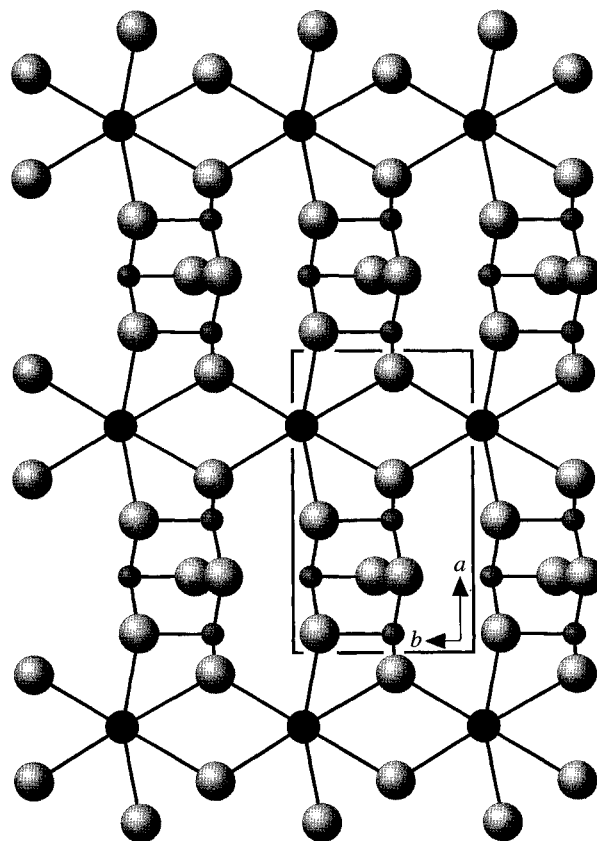
coordinated by S. Bond valences of approximately 0.16 indicate that the As1,3-S4 bonds are real but very weak (Brown, 1974; Brown and Altermatt, 1985). A similar situation is found in the bernardite structure (Pašava et al., 1989), in which two of the As atoms are coordinated by three S atoms at distances ranging from 2.216 to 2.505 Å, with a fourth ranging from 2.986 to 3.088 Å.

In the second type of sheet (Fig. 3), each Tl1 atom is replaced by a pair of edge-sharing AsS₃ pyramids (As4 and As5), which form a chain parallel to [010]. The three-membered rings of AsS₃ pyramids, identical to those found in the first sheet type, are sutured together by corner sharing with these AsS₃ chains. The As4 and As5 pyramids are more regular than those (As1, As2, and As3) that comprise the three-membered pyramidal rings. As4 and As5 also have a distant S4 neighbor, As4-S4 = 3.001 Å and As5-S4 = 2.943 Å. Edge sharing among AsS₃ trigonal pyramids creates an As4-As5 distance of 2.562 Å, which is only slightly longer than the As-As distances in lautite (2.498 Å), CuAsS (Marumo and Nowacki, 1964), and in elemental arsenic (2.51 Å). Electron microprobe analysis,
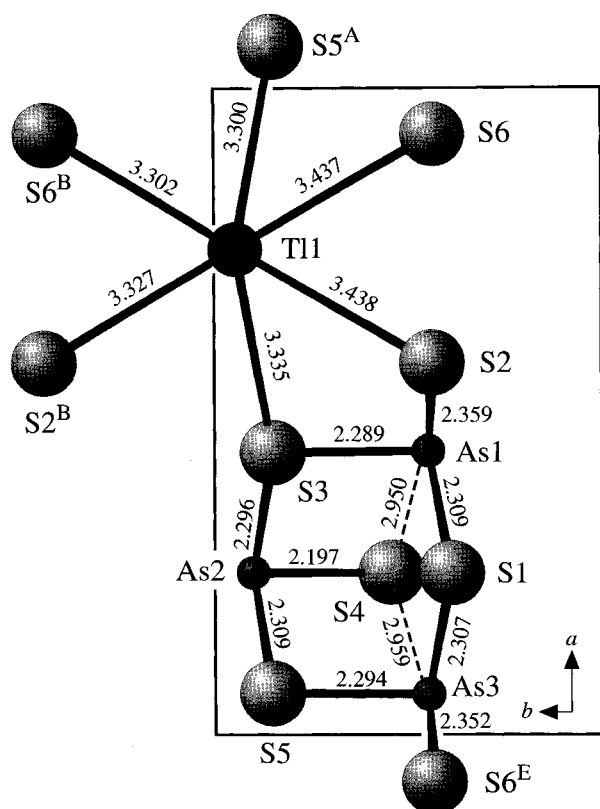
Fig. 2.   The Tl1-As-S sheet projected down [001] showing the bond distances and angles. The unit cell is outlined.

Fig. 3.   The As-S sheet projected down [001] showing the chains of AsS_3 pyramids, the long bonds to S4, and the short As4-As5 distance. The unit cell is outlined.

coupled with site refinement, indicates that 14% of the As4 and 8% of As5 sites are occupied by Sb. Although Sb has a significantly larger covalent radius than As, the mean As4-S and As5-S bond lengths are appreciably shorter (2.269–2.263 Å) than the As1-S, As2-S, and As3-S mean bond lengths (2.267–2.319 Å). In the rebulite structure, $Tl_5Sb_5As_8S_{22}$ (Balić-Žunić and Ščavničar, 1982), there is a partial occupancy of the As site by Sb, and the expected increase in bond length is observed. The shorter than expected As4-S and As5-S mean bond distances in gillulyite may be related to the presence of As4-As5 bonding and interactions between the $4s^2$ lone pair and the bond pair.

Whereas the Tl1 atom is a structural element of only one type of sheet, the Tl2 atom occupies a split position symmetrically displaced about the twofold axis in a large cavity between both types of As-bearing sheets (Figs. 4 and 5). The Tl2 split positions are separated by 1.28 Å, and the occupancy of each is 25%. A similar splitting of the Tl position has been observed in the structure of imhofite (Divjaković and Nowacki, 1976); however, the occupancy is unequal and the split positions are separated by ~0.8 Å. The Tl2 splitting vector lies in the (010) plane approximately 17° to the **a** axis. Because of symmetry constraints on the Tl2 split sites, their S coordinations are identical. Each is coordinated by (6 + 5) S atoms, six
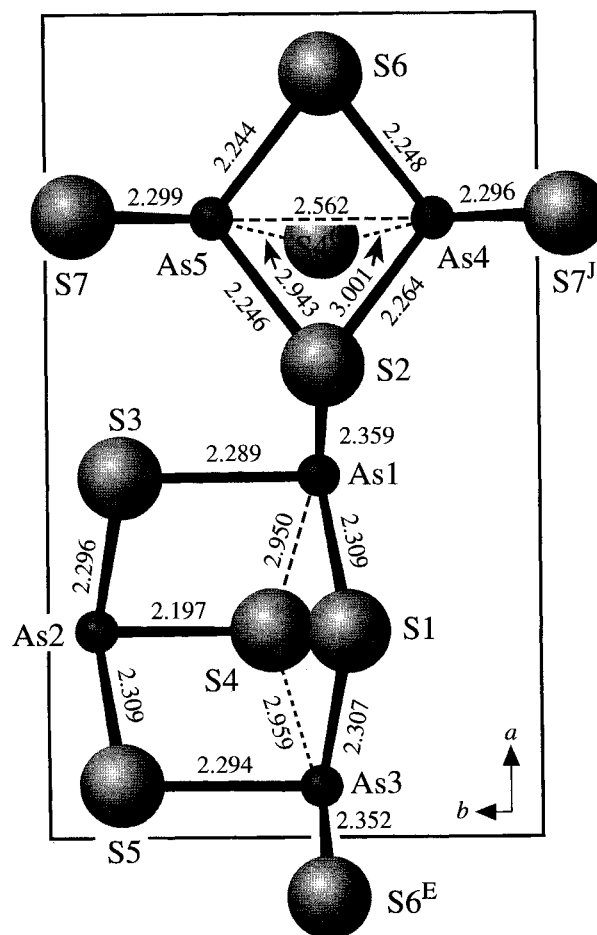
at distances ranging from 3.280 to 3.633 Å and five at distances ranging from 3.860 to 3.971 Å (Table 3). The innermost coordination sphere of six atoms is extremely distorted and displaced away from the adjoining Tl split position. The range of distances of Tl2 to its six closest S neighbors is comparable to those observed in the thallium sulfosalts (e.g., lorandite, bernardite, imhofite). However, as is the case with Tl1 the mean distance (3.445 Å) is slightly longer than for similarly coordinated Tl in sulfosalts. Each Tl2 coordination polyhedron is discrete and does not share polyhedral elements with other Tl polyhedra. There are no Tl-Tl nor Tl-As bonds in the gillulyite structure, as are common in the Tl sulfosalts imhofite (Divjaković and Nowacki, 1976), wallisite (Takéuchi et al., 1968), hatchite (Marumo and Nowacki, 1967), lorandite (Fleet, 1973), synthetic christite (Brown and Dickson, 1976), rebulite (Balić-Žunić and Ščavničar, 1982), vrbaite (Ohmasa and Nowacki, 1971), bernardite (Pašava et al., 1989), and ellisite (Gostojić, 1980).

The Tl2 positions are compatible with either sheet type; therefore, without a careful and very difficult analysis of
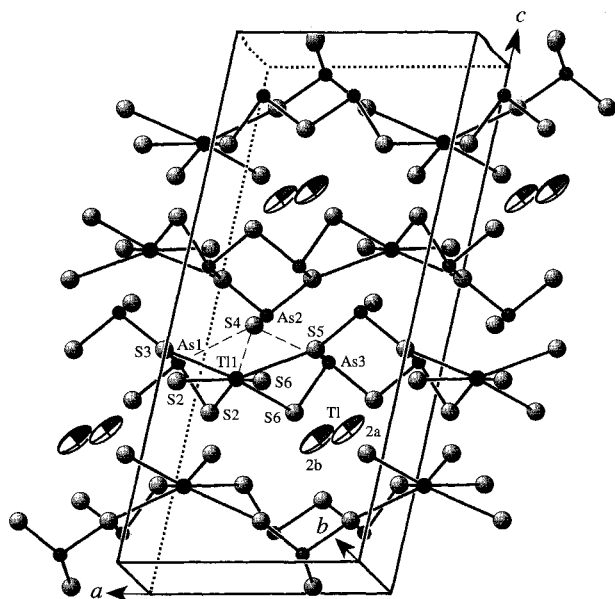
Fig. 4. An oblique view of the gillulyite unit cell showing the stacking of four Tl1-As-S sheets and the split Tl2 position.

Fig. 5. An oblique view of the gillulyite unit cell showing the stacking of four As-S sheets, the split Tl2 position, and the S7-S7 bonds.

the very weak and diffuse extra reflections, it is not possible to determine if Tl2 atoms are ordered (i.e., present with one sheet type) or how the two sheet types are stacked together to produce the superstructure. Thus, the picture we are left with is one of an averaged unit cell in which four sheets stacked parallel to (001) yield the 21 Å c-axis repeat. Each of the two sheet types, Tl1-As-S and As-S, are statistically present one half the time. When the Tl1 atom is present (and all the sheets are of the first type) the pair of sheets in the middle of the unit cell and at the top and bottom (Fig. 4) are linked together by long bonds to S4 from Tl1 (3.915 and 3.983 Å), As1 (2.950 Å), and As3 (2.959 Å) in the adjacent sheet. The presence of these extremely long and very weak bonds explains gillulyite's perfect (001) cleavage. The Tl2 atoms that occupy split positions statistically 25% of the time link the pairs of Tl-As-S sheets together.

When the Tl1 atom is replaced by As4 and As5 pyramids (as it is 50% of the time) the inversion-related pairs of As-S sheets in the middle of the cell are weakly linked together by only the long As1-S4, As3-S4, As4-S4, and As5-S4 bonds (Fig. 5). The S atom (S7), which is part of the coordination spheres of As4 and As5, forms bonds, S7-S7 = 2.24 Å, between the adjacent As-S sheet pairs. In addition to the S-S bonds, the As-S sheet pairs are linked together by Tl2-S bonds.

Covalent S-S bonds have been observed in only a few sulfides and sulfosalts (Wuensch, 1974). The S7-S7 distance in gillulyite is only slightly longer than those in the disulfides, pyrite (2.14 Å) and marcasite (2.21 Å), and in the sulfosalt livingstonite, $HgSb_4S_8$ (2.06 Å) (Srikrishnan and Nowacki, 1975). The presence of S-S and As-As bonds in the same structure has not been observed before in
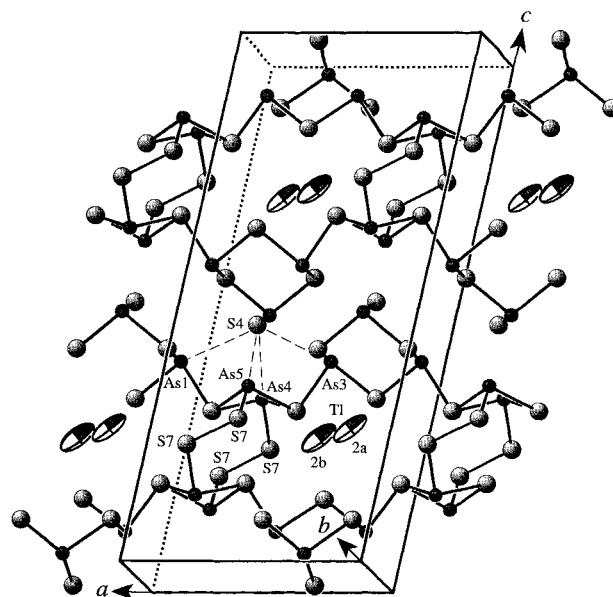
sulfides and sulfosalts; their presence might more appropriately lead to gillulyite being classified as a sulfide (Wuensch, 1974).

Lone pair effects

Gillulyite hosts two cations (As^{3+} and Tl^+), which contain a lone pair of electrons. It is thought that lone pairs (lp) and bonding pairs (bp) "are of equal importance and distribute themselves so as to minimize interelectron repulsion" and that "the repulsion between pairs decreases in the order" lp-lp > lp-bp > bp-bp (Hyde and Andersson, 1989). Since a lone pair of electrons occupies approximately the same volume as an anion "the cation must, therefore, be off-center in the regular polyhedron" (Hyde and Andersson, 1989). As a result, the coordination polyhedra of cations containing a lone pair of electrons in their valence shells are generally extremely distorted, and their interatomic distances vary greatly, making specification of the coordination polyhedron somewhat arbitrary at times.

The coordination of As^{3+} appears to reflect the presence of its $4s^2$ lone pair electrons. The nearly coplanar (001) arrangement of S atoms constituting the AsS_3 pyramids suggests that the lone pair centroids of the As1, As3, As4, and As5 atoms are oriented in the [001] direction, with the lp and three bp pairs having a tetrahedral configuration (Fig. 3). This would place S4 between the lp centroids with the lp-bp (As-S4) repulsions responsible for the dilation of the As-S4 bonds. Likewise the lone pair centroid for the As2 atom probably lies in the void between the As_3S_4 rings and opposes the very short (2.197 Å) As2-S4 bond (Figs. 1 and 3).

Lone pair effects are also evident in Tl coordination

polyhedra, where Tl1-S and Tl2-S distances range from 3.300 to 3.983 Å and 3.280 to 3.971 Å, respectively. Tl1 is displaced to one side of its immediate coordination sphere, with bonds on one side (to S2, S5, and S6) averaging 3.309 Å and those opposing (to S2, S3, and S6) averaging 3.403 Å (Table 3). Although the distortion is compatible with the asymmetric distribution of shared edges in the Tl1 polyhedron (i.e., the bonds to shared edges tend to be the longest), it may also be the product of the orientation of the $6s^2$ lone pair centroid and lp-bp and bp-bp repulsions (Gillespie and Nyholm, 1957; Hyde and Andersson, 1989; Moore and Shen, 1984). In this case the centroid of the lone pair is directed away from the short Tl1-S bonds. A similar severe distortion of the Pb^{2+} coordination polyhedron in roeblingite, Pb_2Ca_6-$(SO_4)_2(OH)_2(H_2O)_4[Mn(Si_3O_9)_2]$ is thought to be due to the $6s^2$ lone pair effect (Moore and Shen, 1984).

The splitting of the Tl2 atom about the twofold axis with a separation of 1.28 Å represents a more interesting lone pair effect, one similar to that exhibited by Pb^{2+} in hyalotekite (Moore et al., 1982), magnetoplumbite (Moore et al., 1989), and kentrolite-melanotekite (Moore et al., 1991). In these structures the Pb centroid is split into as many as six partially occupied sites (magnetoplumbite). Partial ordering of Pb in these sites (kentrolite-melanotekite series) is thought to be responsible for the weak additional reflections and diffuse streaking of the diffraction maxima. Anomalously large residual thermal parameters for Tl2a and Tl2b (Fig. 5) in gillulyite suggest that Tl2 may be split into more than just two sites. Similarly, the partial ordering of Tl1, Tl2, S7, As4, and As5 is probably responsible for the weak and diffuse maxima observed in gillulyite X-ray patterns.

ACKNOWLEDGMENTS

REFERENCES CITED

Balić-Žunić, T., and Šćavničar, S. (1982) The crystal structure of rebulite, $Tl_5Sb_5As_8S_{22}$. Zeitschrift für Kristallographie, 160, 109–125.

Brown, I.D. (1974) Bond valence as an aid to understanding the stereochemistry of O and F complexes of Sn(II), Sb(III), Te(IV), I(V), and Xe(VI). Journal of Solid State Chemistry, 11, 214–233.

Brown, I.D., and Altermatt, D. (1985) Bond valence parameters obtained from systematic analysis of the inorganic crystal structure database. Acta Crystallographica, B41, 244–247.

Brown, K.L., and Dickson, F.W. (1976) The crystal structure of synthetic christite, $HgTlAsS_3$. Zeitschrift für Kristallographie, 144, 367–376.

Divjaković, V., and Nowacki, W. (1976) Die Kristallstruktur von Imhofit, $Tl_{5.6}As_{15}S_{25.3}$. Zeitschrift für Kristallographie, 144, 323–333.

Fleet, M.E. (1973) The crystal structure and bonding of lorandite, $Tl_2As_2S_4$. Zeitschrift für Kristallographie, 138, 147–160.

Gillespie, R.J., and Nyholm, R.S. (1957) Inorganic stereochemistry. Quarterly Review of the London Chemical Society, 11, 339–380.

Gilmore, C.J. (1984) MITHRIL: An integrated direct methods computer program. Journal of Applied Crystallography, 17, 42–46.

Gostojić, M. (1980) Die Kristallstruktur von synthetischem Ellisit, Tl_3AsS_3. Zeitschrift für Kristallographie, 151, 249–254.

Hyde, B.G., and Andersson, S. (1989) Inorganic crystal structures, p. 257–271. Wiley, New York.

Ibers, J.A., and Hamilton, W.C., Eds. (1974) International tables for X-ray crystallography, vol. IV, 366 p. Kynoch, Birmingham, U.K.

Marumo, F., and Nowacki, W. (1964) The crystal structure of lautite and sinnerite, a new mineral from the Lengenbach quarry. Schweizerische mineralogische-petrographische Mitteilungen, 44, 439–454.

——— (1967) The crystal structure of hatchite, $PbTlAgAs_2S_5$. Zeitschrift für Kristallographie, 125, 1–6.

Molecular Structure Corporation (1985) TEXSAN-TEXRAY structure analysis package. MSC, 3200 Research Forest Drive, The Woodlands, Texas.

Moore, P.B., and Shen, J. (1984) Roeblingite, $Pb_2Ca_6(SO_4)_2(OH)_2(H_2O)_4$ $[Mn(Si_3O_9)_2]$: Its crystal strucutre and comments on the lone pair effect. American Mineralogist, 69, 1173–1179.

Moore, P.B., Araki, T., and Ghose, S. (1982) Hyalotekite, a complex lead borosilicate: Its crystal structure and the lone pair effect of Pb(II). American Mineralogist, 67, 1012–1020.

Moore, P.B., Sen Gupta, P.K., and Le Page, Y. (1989) Magnetoplumbite, $Pb^{2+}Fe_{12}^{3+}O_{19}$: Refinement and lone-pair splitting. American Mineralogist, 74, 1186–1194.

Moore, P.B., Sen Gupta, P.K., Shen, J., and Schlemper, E.O. (1991) The kentrolite-melanotekite series, $4Pb_2(Mn,Fe)_2^{3+}O_2[Si_2O_7]$: Chemical crystallographic relations, lone-pair splitting, and cation relation to $8URe_2$. American Mineralogist, 76, 1389–1399.

Ohmasa, M., and Nowacki, W. (1971) The crystal structure of vrbaite $Hg_3Tl_4As_8Sb_2S_{20}$. Zeitschrift für Kristallographie, 134, 360–380.

Pašava, J., Pertlik, F., Stumpfl, E.F., and Zeman, J. (1989) Bernardite, a new thallium arsenic sulphosalt from Allchar, Macedonia, with a determination of the crystal structure. Mineralogical Magazine, 53, 531–538.

Rees, B. (1976) Variance and covariance in experimental electron density studies, and the use of chemical equivalence. Acta Crystallographica, A32, 483–488.

Srikrishnan, T., and Nowacki, W. (1975) A redetermination of the crystal structure of livingstonite, $HgSb_4S_8$. Zeitschrift für Kristallographie, 141, 174–192.

Takéuchi, Y.P., and Sadanaga, R. (1969) Structural principles and classification of sulfosalts. Zeitschrift für Kristallographie, 130, 346–368.

Takéuchi, Y.P., Ohmasa, M., and Nowacki, W. (1968) The crystal structure of wallisite, $PbTlCuAs_2S_5$, the Cu analogue of hatchite, $PbTlAgAs_2S_5$. Zeitschrift für Kristallographie, 127, 349–365.

Wilson, J.R., Robinson, P.D., Wilson, P.N., Stanger, L.W., and Salmon, G.L. (1991) Gillulyite, $Tl_2(As,Sb)_8S_{13}$, a new thallium arsenic sulfosalt from the Mercur gold deposit, Utah. American Mineralogist, 76, 653–656.

Wilson, J.R., Sen Gupta, P.K., Robinson, P.D., and Criddle, A.J. (1993) Fangite, Tl_3AsS_4, a new thallium arsenic sulfosalt from the Mercur Au deposit, Utah, and revised optical data for gillulyite. American Mineralogist, 78, 1096–1103.

Wuensch, B. (1974) Determination, relationships, and classification of sulfide mineral structures. In P.H. Ribbe, Sulfide mineralogy. Mineralogical Society of America Short Course Notes, 1, 2–20.